J Mater Sci: Mater Electron (2015) 26:1858–1865
DOI 10.1007/s10854-014-2621-8

Effect of 0.5 wt% nano-TiO_2 addition into low-Ag Sn0.3Ag0.7Cu solder on the intermetallic growth with Cu substrate during isothermal aging

R. W. Wu · L. C. Tsao · R. S. Chen

Received: 25 September 2014 / Accepted: 15 December 2014 / Published online: 21 December 2014
© Springer Science+Business Media New York 2014

Abstract The interfacial evolution of nano-TiO_2 reinforced low-Ag Sn0.3Ag0.7Cu composite solder on Cu substrate was investigated during 100 and 175 °C isothermal aging for up to 7 days. The thickness of interfacial intermetallic compound (IMC) layers was quantitatively evaluated from SEM micrographs using imaging software. It was found that the mean thickness of interfacial Cu–Sn IMC layers increased linearly with the square root of the aging time. This relationship indicates that the growth of the IMC layer is a diffusion-controlled process. Kinetics analysis shows that the apparent activation energies for the growth of Cu–Sn IMC layers were 40.25 kJ/mol for low-Ag Sn0.3Ag0.7Cu solder and 50.85 kJ/mol for low-Ag Sn0.3Ag0.7Cu composite solder. The reduced diffusion coefficient was proved for the low-Ag Sn0.3Ag0.7Cu composite solder/Cu joints.

1 Introduction

Lead-free Sn–Ag–Cu (SAC) solders have been proposed and widely used as candidates for Ball-Grid-Array (BGA) interconnections in the microelectronic packaging industry due to their relatively good soldering performance, excellent creep resistance, and thermal fatigue reliability, as well as their compatibility with current components [1–3]. However, certain problems remain to be addressed, examples being the formation of coarse pro-eutectic Sn dendrity grains, large plates of Ag_3Sn compounds, and extra growth of interfacial compounds [4]. During the reflowing process, the metallurgical reaction between liquid solder and copper or Ni/Au, or Ag metallization, can result in an intermetallic compound (IMC) layer at the solder/metallization interface, such as both ε-Cu_3Sn and η-Cu_6Sn_5 of Sn solder/Cu [5], Ni_3Sn_4 of Sn solder/Ni [6] and Ag_3Sn of SAC solder/Ag [7]. These IMCs are quite brittle, and excessive thickness can influence the ductility, strength, and reliability of solder joints [8].

Recently, nano-composite solders have been proposed as novel packaging solders that, as compared to conventional lead-free solders, provide excellent properties, such as the microstructures, mechanical properties, wettability, creep resistance, thermo-mechanical fatigue conditions at high temperatures, and suppressed formation or growth of the IMC layer [9–13]. Tsao and Chuang [9] and Tsao et al. [10] demonstrated the influence of reinforcing nano-TiO_2 and -Al_2O_3 particles on the microstructural development and hardness of Sn–Ag–Cu solder alloys. Microhardness measurements revealed that the addition of dioxide nanoparticles enhances the overall strength of the eutectic solder. A similar result was also reported by Tang et al. [11]. Fawzy et al. [12] reported that the addition of nano ZnO particles effectively suppressed the formation, and restricted the volume fraction, of the Ag_3Sn and Cu_6Sn_5 IMC in the SAC355 solder. Gain and Chan [13] showed that Sn–Ag–Cu-1 wt% ZrO_2 composite solder joints exhibited a lower damping capacity than plain SAC solder did due to fine microstructure and uniformly distributed ZrO_2 nanoparticles, which increase the dislocation density. Recently, Tsao and Chen [14] investigated the corrosion property of Cu–Sn IMC in 3.5 wt% NaCl solution and compared it to those of Cu and Sn by using galvanic corrosion and

R. W. Wu · R. S. Chen
Department of Engineering Science, National Cheng Kung University, Tainan 701, Taiwan

L. C. Tsao (✉)
Institute of Materials Engineering, National Pingtung University of Science and Technology, Neipu 91201, Pingtung, Taiwan
e-mail: tlclung@mail.npust.edu.tw

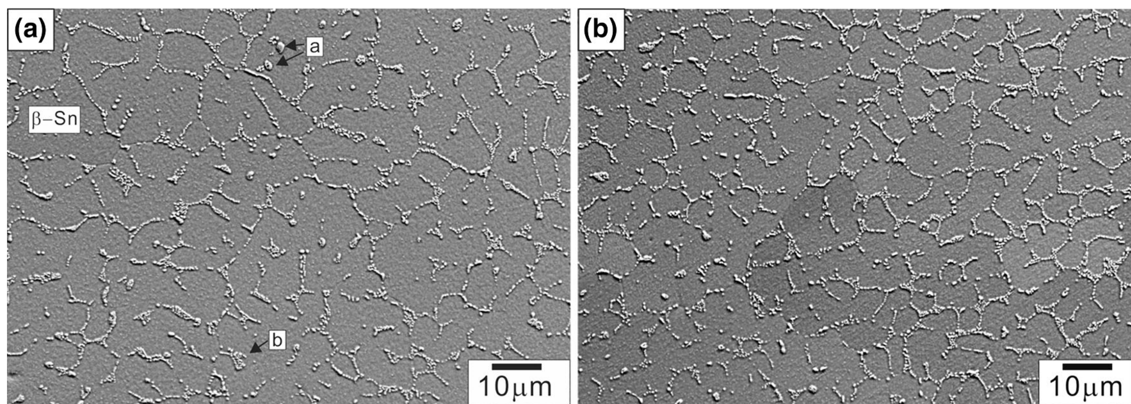

Fig. 1 The microstructure of as-cast low-Ag composite solder: **a** Sn0.3Ag0.7Cu solder; **b** Sn0.3Ag0.7Cu composite solder

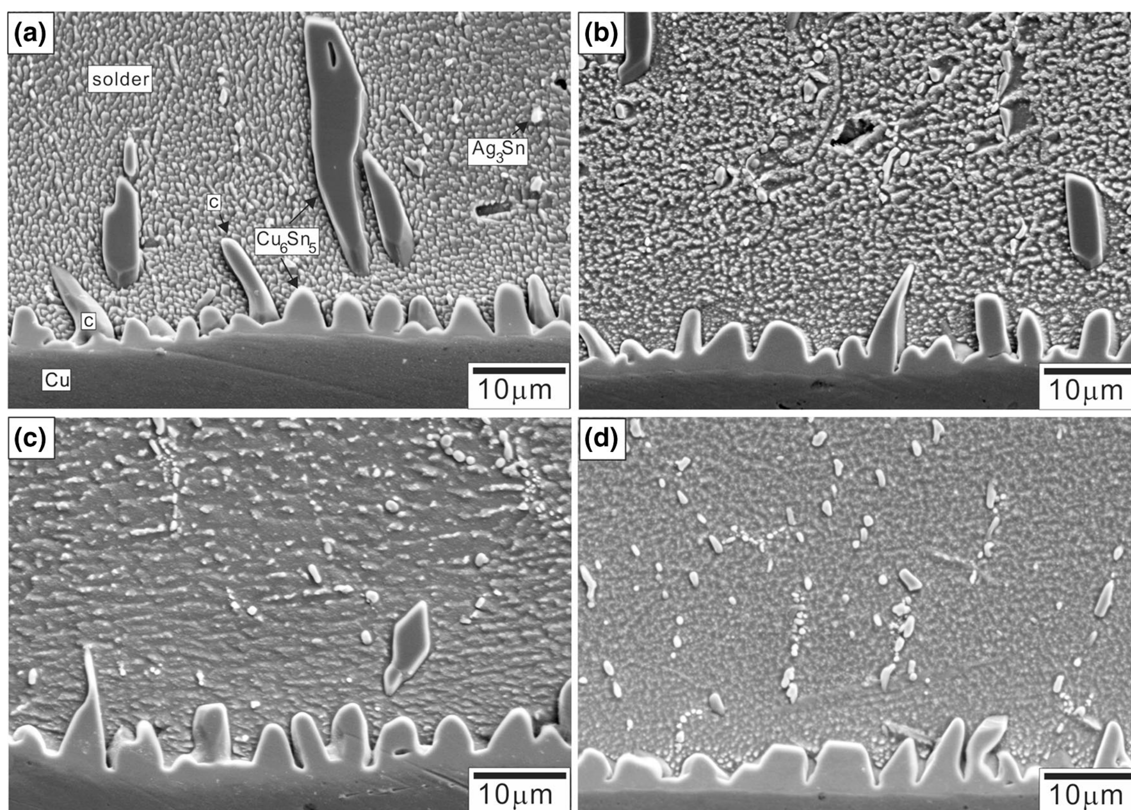

Fig. 2 Cross-section SEM images of the low-Ag Sn0.3Ag0.7Cu solder/Cu interfaces aged at 100 °C for the following times: **a** as-received; **b** 3 days; **c** 5 days; and **d** 7 days

polarization methods. The results showed that an increase in the Cu content increased the corrosion current density (I_{corr}) and shifted both corrosion potential (E_{corr}) and breakdown potential (E_b) towards more noble values. In addition, it is known that during both soldering [15] and aging [16] of SAC composite solder/Cu substrate, Ag_3Sn nanoparticles apparently decrease the surface energy and hinder the growth of the Cu_6Sn5 IMC layer. Gibbs absorption theory can be used to explain the formation of these nanoparticles and their effects on the surface energy of the IMC.

Increased cost concerns over the noble Ag in lead-free Sn–Ag–Cu solders have promoted the development of new low-Ag solder alloys for electronic packaging. El-Daly et al. [17] reported that the addition of nano-silicon carbides into a Sn1Ag0.5Cu solder improved both the microstructure and creep resistance. However, information on the growth kinetics of Cu–Sn IMC in the low-Ag

Sn0.3Ag0.7Cu composite solder/Cu interface during solid-state aging is scarce. This study focuses on the kinetics of the Cu–Sn IMC growth for the low-Ag Sn0.3Ag0.7Cu composite solder/Cu substrate during solid-state aging. The growth rate constants of the IMC were measured as a function of time and temperature, and the activation energy for IMC growth was determined using a diffusion-control growth model.

2 Experimental

2.1 Composite solder

Pure Sn, Ag, and Cu were melted in a vacuum furnace at 600 °C for 2 h to produce solder alloys of low-Ag Sn0.3Ag0.7Cu solder (wt%). The purity of all the materials was 99.99 wt%. The low-Ag Sn0.3Ag0.7Cu composite solders were prepared by mechanically dispersing 0.5 wt% of nano-TiO_2 particles into the low-Ag Sn0.3Ag0.7Cu (wt%) solder with subsequent remelting in a vacuum furnace at 600 °C for 2 h and casting in a mold (size, 8 × 10 × 20 mm). The average diameter of the nominally spherical nano-TiO_2 particles was 20 nm (Nanostructured & Amorphous materials, USA). The ingot was rolled into 1 mm-thick foil.

2.2 Reflowing and aging process

Cu substrates with dimensions of 10 mm × 10 mm were cut from a 1 mm-thick Cu plate (3N5), ground with SiC paper, and polished with 1 and 0.3 μm Al_2O_3 powders. The low-Ag Sn0.3Ag0.7Cu composite solder/Cu joint samples were prepared by reflowing process. Low-Ag Sn0.3Ag0.7Cu solder sheets and Cu plates were ultrasonically cleaned in ethanol before soldering. Rosin mildly activated (RMA) flux was used in this reflowing process. The substrates were heated on a hot plate to 30 °C above the melting temperature of the low-Ag Sn0.3Ag0.7Cu solder (about $T_m = 213.9$ °C), and the temperature was kept stable, within ±3 °C. Each reaction couple was then placed in an oven maintained at a constant aging temperature. Accelerated aging was performed in air furnaces with a temperature control of ±0.5 °C. The aging temperatures were 100, 125, 150, and 175 °C. The time periods were 1–7 days, with a tracking error of ±30 min.

2.3 Morphology and growth kinetics analysis

The specimens were cross-sectioned, ground with SiC paper, polished with 1 and 0.3 μm Al_2O_3 powders, and etched with 5 % HCl and 95 % H_2O solution. The morphologies were studied using a scanning electron microscope (SEM, s-3000H, Hitachi Co.) with a voltage of 20 keV. The chemical compositions of the IMCs were analyzed by energy-dispersion spectroscopy (EDS). X-ray diffraction (XRD, D/max 2500 V/PC) was used to analyze the phase. The polished cross-sections of the low-Ag composite solder/Cu substrate diffusion couples were examined by SEM, and the digitally captured micrographs were semi-automatically processed using the Image-Pro software to determine the average thickness (X) of the IMC layer. Five micrographs were used for each inter-diffusion experimental condition. The average IMC layer thickness (x) was measured by using the following formula:

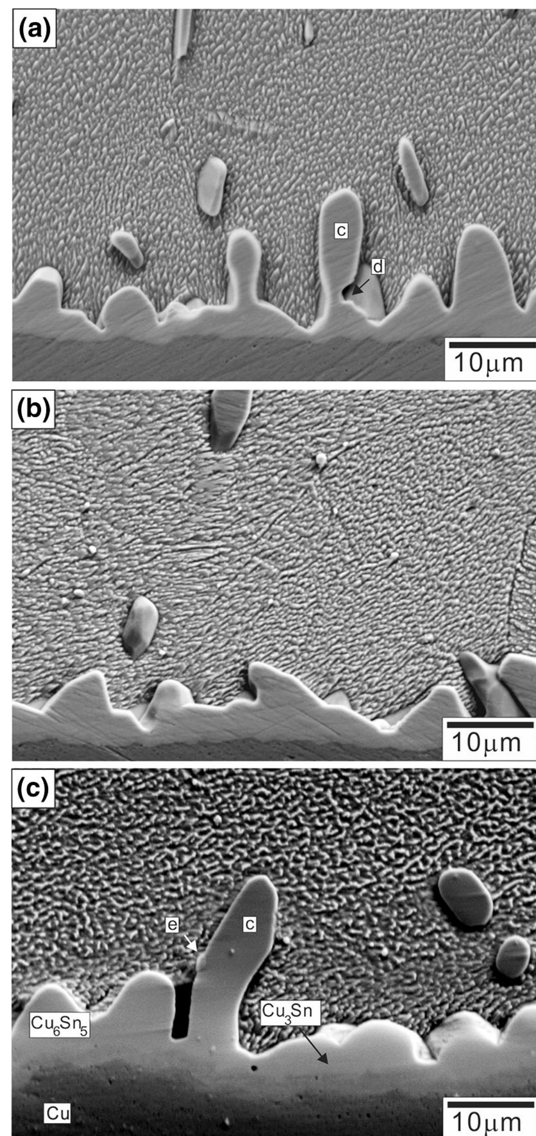

Fig. 3 Cross-section SEM images of the low-Ag Sn0.3Ag0.7Cu solder/Cu interfaces aged for 7 days at different temperatures: **a** 125 °C; **b** 150 °C; and **c** 175 °C

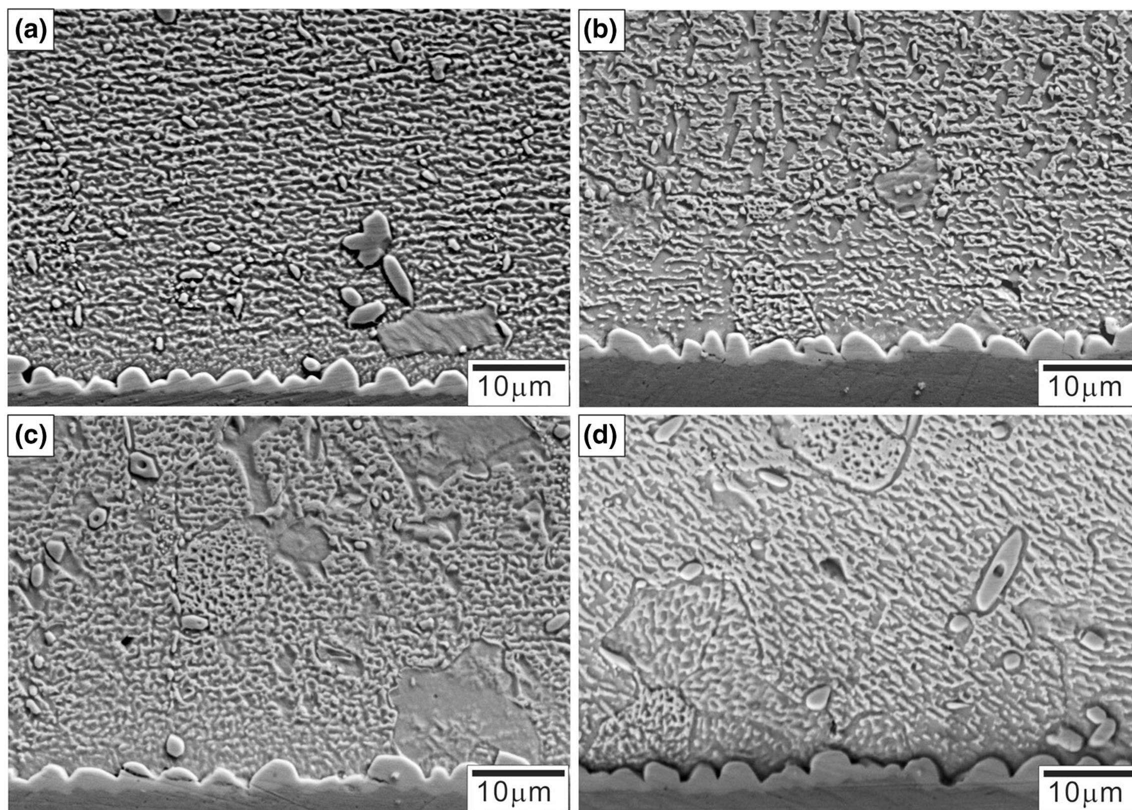

Fig. 4 Cross-section SEM images of the low-Ag Sn0.3Ag0.7Cu–0.75TiO_2 composite solder/Cu interfaces aged at 100 °C for the following times: **a** as-received; **b** 3 days; **c** 5 days; and **d** 7 days

$$X = S/L \quad (1)$$

where L is the length measured, and S is the integral contour area of the IMC layer at the low-Ag composite solder/Cu interface.

3 Results and discussion

3.1 Microstructure of low-Ag Sn0.3Ag0.7Cu composite solder

The addition of nano-TiO_2 particles into the low-Ag Sn0.3Ag0.7Cu solder influences the final microstructures significantly. Figure 1 is an SEM micrograph of the as-cast low-Ag Sn0.3Ag0.7Cu composite solder. The plain low-Ag Sn0.3Ag0.7Cu solder contains dendritic β–Sn with a size of 8.6 ± 2.3 μm, a small particle of Cu_6Sn_5 (mark a), and a eutectic area (mark b) where the Cu_6Sn_5 phase is finely dispersed. However, the course Ag_3Sn plate was not observed in the low-Ag Sn0.3Ag0.7Cu solder. Addition of nano-TiO_2 particles was observed to reduced the grain size of dendritic β–Sn (4.9 ± 1.8 μm) in the low-Ag Sn0.3Ag0.7Cu composite solder. However, both the grain size and the amounts (i.e., volume fraction) of Cu_6Sn_5 phase in the eutectic area were similar in the low-Ag Sn0.3Ag0.7Cu solder.

3.2 Microstructure of interfacial IMC layers

Figure 2 shows the interfacial microstructure of the low-Ag Sn0.3Ag0.7Cu solder/Cu joints. In the as-soldered joints, the IMC layer was mainly the discontinuous sharp-hill Cu_6Sn_5 layer at the low-Ag Sn0.3Ag0.7Cu solder/Cu interface (Fig. 2a). The EDS analysis reveals that the interfacial IMC layer consisted of only one layer of Cu_6Sn_5 phase. The chemical composition (wt%) was Cu:Sn = 59.97:41.03. In addition, both coarse, gray Cu_6Sn_5 and fine, white Ag_3Sn were observed in the low-Ag Sn0.3Ag0.7Cu solder area. Also, the wicker-Cu_6Sn_5 formed on the Cu_6Sn_5 layer (mark c) and grew into the solder matrix. This result is in good agreement with previously reported results [7].

After isothermal aging, the IMC layer in all solders became thicker and formed a plateau (Figs. 2, 3). The inner Cu_3Sn layer was obvious in the low-Ag Sn0.3Ag0.7Cu solder/Cu interfaces aged for 7 days at 175 °C (Fig. 3c). In Fig. 3a, it is interesting that the neck of wicker-Cu_6Sn_5 for Sn0.3Ag0.7Cu solder/Cu gradually shrank (mark d). In

previous work, it was clearly reported that the wicker-Ag_3Sn broke off or dissolved into the matrix and IMC grains tended to form the scallop-type morphologies in the Sn3.5Ag0.5Cu solder/Ag joints [7]. This suggests that a substantial neck of wicker-Ag_3Sn might dissolve into molten solder prior to the formation of the intermetallic layer. In another study, Liu et al. [18] reported that the longer stick-shaped Cu_6Sn_5 IMC growth on the Cu_6Sn_5 interfacial layer and dissolved, broke off, and shifted to the solder matrix. The wicker-IMC caused a high stress concentration focus and original cracks to form. Thus, the wicker-IMC would be harmful to the reliability of the solder joints [19]. Also, Ag_3Sn particles (mark e) were embedded in the Cu_6Sn_5 IMC, as shown in Fig. 3c. This observation is consistent with a previous study on the intermetallic growth in both Sn–Ag/Cu [20–23] and Sn3.5G0.5Cu/Ag [7] interfacial reactions. This suggests that Ag_3Sn particles retarded the growth of Cu_6Sn_5 IMC.

Figure 4 shows an SEM micrograph of IMC layers for the Sn0.3Ag0.7Cu composite solder/Cu joints. Compared to the Sn0.3Ag0.7Cu solder/Cu joints (Fig. 2a), the Sn0.3Ag0.7Cu composite solder/Cu interface exhibited a discontinuous scallop-shaped Cu_6Sn_5 IMC layer (Fig. 4a). In the isothermal aging process, it was found that the Cu_6Sn_5 IMC layer at the interface had, overall, gradually transformed from the discontinuous scallop-type to the planar-type in the Sn0.3Ag0.7Cu composite solder joints (Figs. 4, 5). In addition, both the wicker- and coarse-Cu_6Sn_5 IMCs were not observed in the Sn0.3Ag0.7Cu composite solder matrix after solid-state aging. This difference in morphology indicates that the addition of nano-TiO_2 particles to the Sn0.3Ag0.7Cu solder can affected the morphology of the IMC layer that forms [16, 24].

3.3 Growth kinetic

The variation in thickness of the IMC layer (ΔX) of low-Ag Sn0.3Ag0.7Cu composite solder/Cu at different aging temperatures (Fig. 6) shows a linear relationship between IMC thickness and aging time ($h^{1/2}$). This relationships indicates that the growth of Cu–Sn IMCs during the interfacial reactions between low-Ag Sn0.3Ag0.7Cu composite solder and Cu substrates is diffusion-controlled. Many researchers have reported that the kinetics of IMC growth can be diffusion-controlled [24, 25].

The temperature variations of D for the IMC layer growth can be expressed by the following Arrhenius equation in terms of the interdiffusion coefficient [26]:

$$X_t = X_o + \sqrt{Dt} \tag{2}$$

$$D = D_0 \exp\left(\frac{-Q}{RT}\right) \tag{3}$$

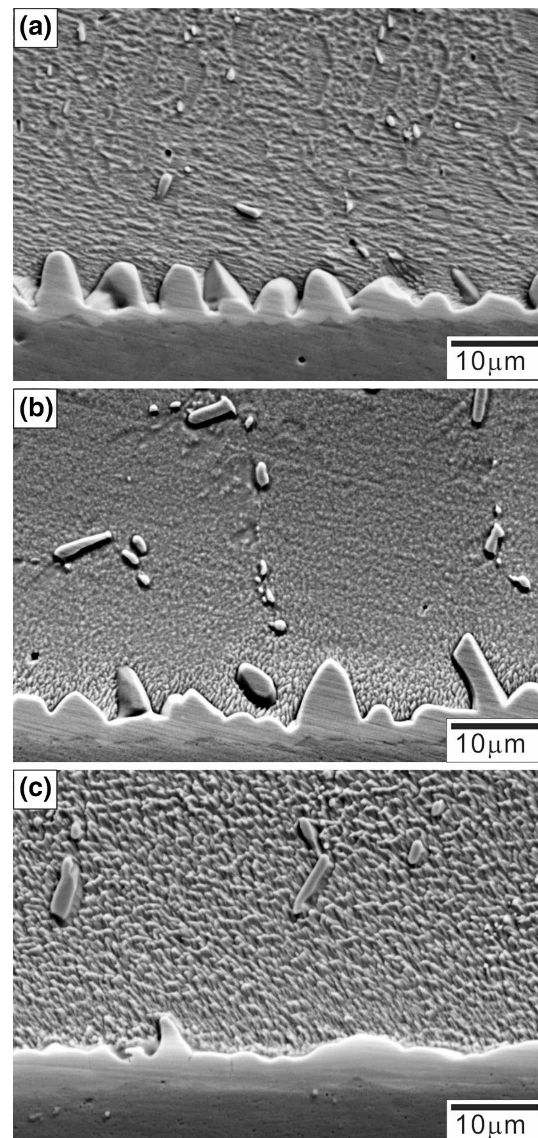

Fig. 5 Cross-section SEM images of the low-Ag Sn0.3Ag0.7Cu–0.75TiO_2 composite solder/Cu interfaces aged for 7 days at different temperatures: **a** 125 °C; **b** 150 °C; and **c** 175 °C

where X_t is the IMC thickness (m) at isothermal aging time t, X_o is the initial thickness (m) after soldering, D is the diffusion coefficient (m^2/s), D_0 is the interdiffusion constant (m^2/s), Q is activation energy (kJ/mol) for the growth of the interfacial IMC layer, R is the gas constant, and T is the absolute temperature. The growth rate constants ($D = x^2/t$), in turn, were then used to calculate the activation energies from Eq. 3 using linear regression analysis of a plot of ln(D) versus (1/T). An Arrhenius plot of the growth rate constants versus reaction temperature is shown in Fig. 7. The diffusion coefficients, D, for growth of the Cu–Sn IMC layer in the low-Ag Sn0.3Ag0.7Cu solder and low-Ag Sn0.3Ag0.7Cu composite solder joints at different

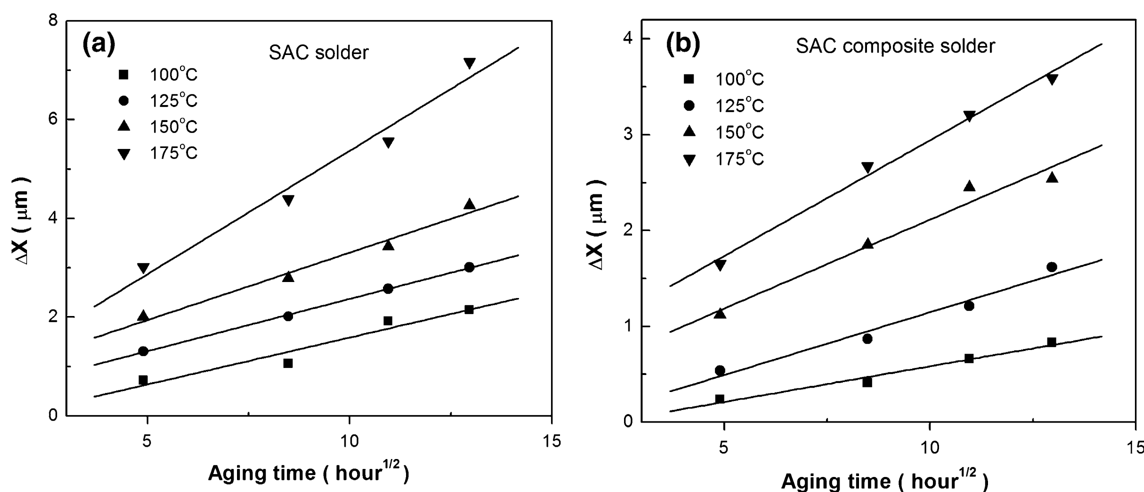

Fig. 6 The relationship curves between IMC thickness, aging temperature, and aging time ($h^{1/2}$) for low-Ag Sn0.3Ag0.7Cu solder/Cu (**a**) and low-Ag Sn0.3Ag0.7Cu composite solder/Cu (**b**) during isothermal aging

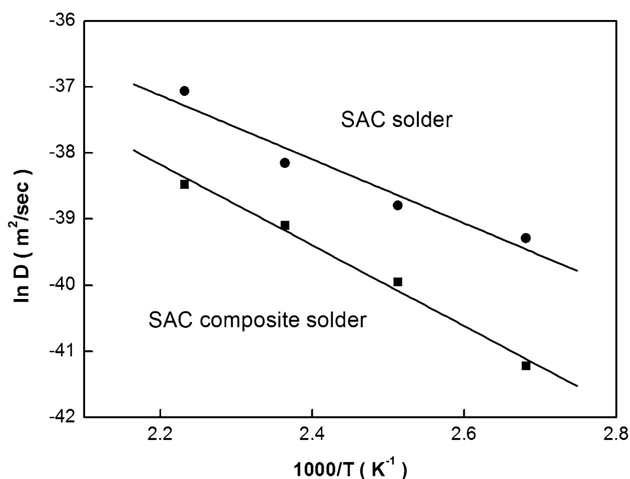

Fig. 7 Arrhenius plot of overall IMC layer formed by low-Ag Sn0.3Ag0.7Cu solder/Cu and low-Ag Sn0.3Ag0.7Cu composite solder/Cu

aging temperatures are shown in Table 1. From Eq. (3) and the data in Fig. 7, the diffusion constants were calculated to be 3.18×10^{-12} and 1.84×10^{-11} m^2/s for low-Ag Sn0.3Ag0.7Cu and low-Ag Sn0.3Ag0.7Cu composite solders, respectively. The activation energies for the growth of the interfacial Cu–Sn IMC layer during isothermal aging process are estimated to be 40.25 kJ/mol for low-Ag Sn0.3Ag0.7Cu solder/Cu and 50.85 kJ/mol for low-Ag Sn0.3Ag0.7Cu composite solder/Cu. The low-Ag Sn0.3Ag0.7Cu composite solder joints exhibited lower diffusion coefficients than did the low-Ag Sn0.3Ag0.7Cu solder joint. Therefore, the composite solder joints were also effective in retarding the growth of the Cu_6Sn_5 IMC layer. In previous work, the apparent activation energies for the growth of Cu–Sn IMC layers were calculated as 42.48 kJ/mol for high-Ag Sn3.5Ag0.5Cu solder and 60.31 kJ/mol for high-Ag Sn3.5Ag0.5Cu composite solder

Table 1 Calculated diffusion coefficients and activation energies of overall IMCs for low-Ag Sn0.3AgAg0.5Cu solder/Cu and low-Ag Sn0.3Ag0.5Cu composite solder/Cu reaction couples during isothermal aging

Reactive couples	Temperature (°C)	Diffusion coefficient $D(\times 10^{-18}, m^2/s)$	Diffusion constant D_0 (m^2/s)	Activation energy Q (KJ/mol)	Reference
Sn0.3Ag0.7Cu/Cu	100	8.61	3.18×10^{-12}	40.25	
	125	14.24			
	150	26.94			
	175	80.15			
Sn0.3Ag0.7Cu–0.5TiO_2/Cu	100	1.25	1.84×10^{-11}	50.85	
	125	4.46			
	150	10.52			
	175	19.49			
Sn3.5Ag0.5Cu/Cu	100–175	–	3.25×10^{-12}	42.48	[16]
Sn3.5Ag0.5Cu-0.5 TiO_2/Cu	100–175	–	2.53×10^{-10}	60.31	[16]

[16]. It has been reported that nano-TiO_2 particles affect the growth patterns of the IMC layers and that advanced nano-Ag_3Sn particles are absorbed in the surface of Cu_6Sn_5 layer during aging of the Sn3.5Ag0.5Cu composite solder/Cu [15, 16]. These phenomena suggest that the low-Ag composite solder did not form a large amount of nano-Ag_3Sn particles. As a result, nano-Ag_3Sn particles absorbed in the Cu_6Sn_5 surface and thereby suppress IMC growth. This indicates that intermixing of nano-TiO_2 particles in the low-Ag Sn0.3Ag0.7Cu solder joints was mainly effective in retarding the growth of the IMC layer.

4 Conclusions

In this research, the formation and the growth of the Cu–Sn IMC layer in the low-Ag Sn0.3Ag0.7Cu composite solder/Cu interface during aging were studied. In the low-Ag Sn0.3Ag0.7Cu solder/Cu joints, both the discontinuous sharp-hill Cu_6Sn_5 layer and the wicker-Cu_6Sn_5 formed on the Cu_6Sn_5 layer were observed in the as-soldered joints. After isothermal aging, the IMC layer in all solders became thicker and plateau. However, in the Sn0.3Ag0.7Cu composite solder/Cu joints, a discontinuous scallop-shaped Cu_6Sn_5 layers were found at Sn0.3Ag0.7Cu/Cu interfaces after soldering, These layers gradually grew planar-like after isothermal aging. Based on Arrhenius plots, the activation energies of Cu–Sn IMC layer growth were calculated as 40.25 and 50.85 kJ/mol for the low-Ag Sn0.3Ag0.7Cu solder and low-Ag Sn0.3Ag0.7Cu composite solder joints, respectively. These calculations confirmed that intermixing of nano-TiO_2 particles in the low-Ag Sn0.3Ag0.7Cu solder joints was mainly effective in retarding the growth of the IMC layer.

Acknowledgments The authors acknowledge the financial support of this work by the National Science Council of the Republic of China under Project No. NSC 97-2218-E-020-004. SEM was performed by the Precision Instrument Center of National Pingtung University of Science and Technology, Taiwan.

References

1. I. Anderson, Development of Sn–Ag–Cu and Sn–Ag–Cu–X alloys for Pb-free electronic solder applications. J. Mater. Sci. Mater. Electron. **18**, 55–76 (2007)
2. W.P. Liu, N.C. Lee, The effects of additives to SnAgCu alloys on microstructure and drop impact reliability of solder joints. JOM, **59**, 26–31 (2007)
3. L M. Lee, A.A. Mohamad, Interfacial reaction of Sn–Ag–Cu lead-free solder alloy on Cu: a review. Adv. Mater. Sci. Eng. **2013**, 1–11 (2013)
4. D.W. Henderson, T. Gosselin, A. Sarkhel, S.K. Kang, W.K. Choi, D.Y. Shih, C. Goldsmith, K.J. Puttlitz, Ag_3Sn plate formation in the solidification of near ternary eutectic Sn–Ag–Cu alloys. J. Mater. Res. **17**, 2775–2778 (2002)
5. S.Y. Chang, C.C. Jain, T.H. Chuang, L.P. Feng, L.C. Tsao, Effect of addition of TiO_2 nanoparticles on the microstructure, microhardness and interfacial reactions of Sn3.5AgXCu Solder. Mater. Des. **32**, 4720–4727 (2011)
6. J. Görlich, D. Baither, G. Schmitz, Reaction kinetics of Ni/Sn soldering reaction. Acta Mater. **58**, 3187–3197 (2010)
7. R.W. Wu, L.C. Tsao, S.Y. Chang, C.C. Jain, R.S. Chen, Interfacial reactions between liquid Sn3.5Ag0.5Cu solders and Ag Substrates. J. Mater. Sci. Mater. Electron. **22**, 1181–1187 (2011)
8. J. Bertheau, F. Hodaj, N. Hotellier, J. Charbonnier, Effect of intermetallic compound thickness on shear strength of 25 μm diameter Cu-pillars. Intermetallics **51**, 37–47 (2014)
9. L.C. Tsao, S.Y. Chuang, Effects of nano-TiO_2 additions on thermal analysis, microstructure and tensile properties of Sn3.5Ag0.25Cu solder. Mater. Des. **31**, 990–993 (2010)
10. L.C. Tsao, S.Y. Chang, C.I. Lee, W.H. Sun, C.H. Huang, Effects of nano-Al_2O_3 additions on microstructure development and hardness of Sn3.5Ag0.5Cu solder. Mater. Des. **31**, 4831–4835 (2010)
11. Y. Tang, G.Y. Li, Y.C. Pan, Effects of TiO_2 nanoparticles addition on microstructure, microhardness and tensile properties of Sn–3.0Ag–0.5Cu–$x$$TiO_2$ composite solder. Mater. Des. **55**, 574–582 (2014)
12. A. Fawzy, S.A. Fayek, M. Sobhy, E. Nassr, M.M. Mousa, G. Saad, Tensile creep characteristics of Sn3.5Ag0.5Cu (SAC355) solder reinforced with nano-metric ZnO particles. Mater. Sci. Eng. A **603**, 1–10 (2014)
13. A.K. Gain, Y.C. Chan, Growth mechanism of intermetallic compounds and damping properties of Sn–Ag–Cu–1 wt% nano-ZrO_2 composite solders. Microelectron. Rel. **54**, 945–955 (2014)
14. L.C. Tsao, C.W. Chen, Corrosion characterization of Cu–Sn intermetallics in 3.5 wt% NaCl solution. Corros. Sci. **63**, 393–398 (2012)
15. L.C. Tsao, Evolution of nano-Ag_3Sn particle formation on Cu–Sn intermetallic compounds of Sn3.5Ag0.5Cu composite solder/Cu during soldering. J. Alloys Compd. **509**, 2326–2333 (2011)
16. L.C. Tsao, Suppressing effect of 0.5 wt% nano-TiO_2 addition into Sn–3.5Ag–0.5Cu solder alloy on the intermetallic growth with Cu substrate during isothermal aging. J. Alloys Compd. **509**, 8441–8448 (2011)
17. A.A. El-Daly, G.S. Al-Ganainy, A. Fawzy, M.J. Younis, Structural characterization and creep resistance of nano-silicon carbide reinforced Sn–1.0Ag–0.5Cu lead-free solder alloy. Mater. Des. **55**, 837–845 (2014)
18. X.Y. Liu, M.L. Huang, Y.H. Zhao, C.M.L. Wu, L. Wan, The adsorption of Ag_3Sn nano-particles on Cu–Sn intermetallic compounds of Sn–3Ag–0.5Cu/Cu during soldering. J. Alloys Comp **492**, 433–438 (2010)
19. A. Sharif, Y.C. Chan, Effect of Indium addition in Sn-rich solder on the dissolution of Cu metallization. J. Alloys Compd. **390**, 67–73 (2005)
20. S. Choi, J.P. Lucas, K.N. Subramanian, T.R. Bieler, Formation and growth of interfacial intermetallic layers in eutectic Sn–Ag solder and its composite solder joints. J. Mater. Sci. Mater. Electron. **11**, 497–502 (2000)
21. S. Choi, T.R. Bieler, J.P. Lucas, K.N. Subramanian, Characterization of the growth of intermetallic interfacial layers of Sn–Ag and Sn–Pb eutectic solders and their composite solders on Cu substrate during isothermal long-term aging. J. Electron. Mater. **28**, 1209–1215 (1999)
22. D.R. Flanders, E.G. Jacobs, R.F. Pinizzotto, Activation energies of intermetallic growth of Sn–Ag eutectic solder on copper substrates. J. Electron. Mater. **26**, 883–887 (1997)
23. J.W. Yoon, S.B. Jung, Effect of isothermal aging on intermetallic compound layer growth at the interface between Sn–3.5Ag–0.75Cu solder and Cu substrate. J. Mater. Sci. **39**, 4211–4217 (2004)

24. S.Y. Chang, L.C. Tsao, M.W. Wu, C.W. Chen, The morphology and kinetic evolution of intermetallic compounds at Sn–Ag–Cu solder/Cu and Sn–Ag–Cu-0.5Al_2O_3 composite solder/Cu interface during soldering reaction. J. Mater. Sci. Mater. Electron. **23**, 100–107 (2012)
25. L.C. Tsao, C.P. Chu, S.F. Peng, Study of interfacial reactions between Sn3.5Ag0.5Cu composite alloys and Cu substrate. Microelectron. Eng. **88**, 2964–2969 (2011)
26. R.J.K. Wassink, *Soldering in Electronics* (Electrochemical Publications Ltd., Ayr, 1989), pp. 149–159